J. Water Environ. Nanotechnol., 9(1): 90-98 Winter 2024

ORIGINAL RESEARCH PAPER

Biosynthesis of αMnO_2 nanorods using coleus amboinicus leaf extract and its adsorption performance of Pb(II) from aqueous solutions

Rejani Padmavathiamma [1], Rani Kunjiraman Pillai [2]*

[1] *Department of Chemistry, NSS College Nilamel, University of Kerala ,Kerala ,India*
[2] *Department of Physics, NSS college Nilamel, University of Kerala, Kerala ,India*

Received: 2023-10-02 Accepted: 2023-12-25 Published: 2024-01-31

ABSTRACT
Heavy metals are known to be toxic for living organisms even if they are present at low levels. Water pollution by heavy metals from industries is a dangerous environmental problem. Due to the ease, flexibility, and cost-effectiveness of the remediation process, adsorption has been widely implemented in heavy metal wastewater treatment. In the present study, nanostructured manganese oxide was used for the removal of the heavy metal ions from aqueous solutions by a batch adsorption method and has been modeled using classical Langmuir and Freundlich adsorption isotherms. we have successfully synthesized an efficient adsorbent through a cost-effective and eco-friendly method. Biosynthesis is widely applied for the synthesis of nanomaterials. Various techniques such as XRD, FTIR, SEM EDX, TEM, and UV–VIS spectroscopy have been used to characterize the nano metal oxide. The obtained nano manganese oxide rods have very good adsorption efficiency due to the presence of some functionalities associated with the oxide material

Keywords: *Adsorption; Langmuir and Freundlich Isotherms; Heavy Metals; Nanostructured Manganese Oxide*

How to cite this article
Padmavathiamma R., Pillai R. K., Biosynthesis of αMnO_2 nanorods using Coleus amboinicus leaf extract and its adsorption performance of Pb(II) from aqueous solutions. J. Water Environ. Nanotechnol., 2024; 9(1): 90-98.
DOI: 10.22090/jwent.2024.01.06

INTRODUCTION

The green method of synthesis of nanoparticles has been noticed due to cost-effectiveness, environmental benefits, and less time duration compared with conventional physical, chemical, and hybrid methods. Biosynthesized nanoparticles especially metal oxides show catalysis, optics, magnetic,photo-electrochemical, and magnetic properties [1],[2]. Green synthesis of metal oxide nanoparticles using plant extract has been reported by several workers. Shende A reported biosynthesized iron oxide nanoparticle from plant-based bio flocculant extracted from the fruits of Okra(Abelmoschus esculentus) was used for lead adsorption [3]. In addition, Sindhudevi et al synthesized Selenium/Zirconium bimetallic nanoparticles using Cinnamomum camphora leaf extract and studied the photocatalyst and anticancer activity [4].

In the past years, the removal of heavy metals from wastewater streams has been widely studied due to the hazard of such pollutants to public health and the environment. The contamination of divalent metal ions is a major problem in many industrial areas, such as fertilizer industries, tanneries, metal plating facilities, batteries, paper industries, and pesticides. Heavy metal wastewaters are directly or indirectly discharged into the environment increasingly, remarkably in developing countries. Since heavy metal ions threaten both human health and the ecosystem their removal from water is highly desirable [5]. With

* Corresponding Authors Email: *rejanihari82@gmail.com*

the development of stringent ecological standards, these industries must reduce the amount of heavy metal ions in their effluents to an acceptable level before discharging into municipal sewers. Various methods have been developed to remove lead and chromium from industrial wastewater, such as ion exchange and reverse osmosis. However, these methods have many drawbacks. Both ion exchange and reverse osmosis methods are not economically attractive because of their high operating costs. Recently, adsorption has been recognized as one of the best techniques for this purpose. [6-9]. Manganese oxides are largely used in adsorption of removing Pb(II) from aqueous solutions. However, according to some

recent studies, the adsorption affinity of MnO_2 towards Pb(II) was highly related to the structures and surface properties of MnO_2. Zhang et al studied the adsorptive removal of Pb (II) using various crystalline structures of manganese oxide and found the following order of δ-MnO_2 >α-MnO_2 > λ-MnO_2 >γnO_2 > β-MnO_2 [10].

Huang et al studied Pb(ii) adsorption by MnO_2/MgFe-layered double hydroxide (MnO_2/MgFe-LDH) and MnO_2/MgFe-layered metal oxide (MnO_2/MgFe-LDO) and found that the optimum adsorption capacity for Pb(II) was achieved at the calcination temperature of 400 °C for MnO_2/MgFe-LDH. Langmuir and Freundlich adsorption isotherm models, pseudo-first-order and pseudo-second-order kinetics, Elovich model, and thermodynamic studies were used for exploring the Pb(II) adsorption mechanism of the two composites. Through characterization analysis, they found the main mechanisms involved in the adsorption process were precipitation action, complexation with functional groups, electrostatic attraction, cation exchange and isomorphic replacement, and memory effect [11].

In this study biosynthesised αMnO$_2$ was used as an adsorbent material for the removal of Pb(II) which is commonly present in industrial effluents. Synthesised material was well characterized by different experimental techniques like XRD, FTIR, UV Visible Spectroscopy, SEM, and TEM. The adsorption efficiency of the material was studied using Atomic Absorption Spectroscopy (AAS) [12-18].

EXPERIMENTAL METHOD

Materials

Fresh leaves of Coleus amboinicus were collected from Nilamel, Kollam district, Kerala, India. The plant material was examined for infections and insect damage and washed at room temperature. All the chemicals and reagents used were of analytical grade. Potassium permanganate (Emplura, Merck Life Science Pvt. Limited), Lead nitrate Hexahydrate purchased from NICE chemicals without any other prior treatment is used for preparing the stock.

Synthesis of nanoparticles

The leaf extract was prepared by boiling 200 g of fresh leaf of Coleus amboinicus in 200 mL of distilled water and the boiling was continued to obtain a dark brown colour extract solution. The filtered plant extract was made up to 500 mL with distilled water, then 20 mL of 0.1 M $KMnO_4$ solution was added and stirred for two hours using a magnetic stirrer [19,20]. A brown-colored precipitate was obtained. The reaction mixture was filtered, and washed with deionized water to obtain pure manganese oxide nanoparticles dried at 400°C for 2 h and used for further characterization.

Characterization of MnO_2 nanoparticles

The synthesized MnO_2 nanoparticles were subjected to various spectral studies such as particle size analyzer, FT-IR, XRD, SEM, and TEM analyses. Fourier transform measurements were taken by using a Fourier transform infrared spectrophotometer (Thermo Scientific, Nicolet iS50). Powder X-ray diffraction measurements were taken using an X-ray diffractometer (DST-SAIF Cochin). TEM images were recorded by using a JEOL/JEM 2100 (DST-SAIF Cochin). UV–visible absorption measurements were taken by a UV–VIS–NIR spectrophotometer (Agilent Technologies, Cary 5000). Adsorption studies were carried out using Atomic Absorption Spectroscopy (AAS).

Adsorption study

The adsorption batch experiments were conducted using a rotary shaker in the absence of sunlight to avoid the degradation of pollutants and to ensure the conditions to attain Adsorption-Desorption equilibria. For a better understanding of the adsorption affinity of adsorbent adsorption media is decanted in the form of small aliquots and the concentrations of adsorbate in the same are determined by an instrument called Atomic Absorption Spectrometer. (GBC-AAS

spectrometer). The mass balance equation can be used for calculating the adsorption efficiency of adsorbate towards the presence of Pb^{2+} ions in the aqueous phase. The mass balance equation for the same can be represented as

$$q_e = \frac{(C0 - Ce)V}{m} \quad (1)$$

Where qe is called the amount of adsorbed Lead ions such as Pb2+ on the surface sites of adsorbent per mg/g. m is the total amount of adsorbent used for the analysis, m is the total amount of absorbent taken for the study, V is the total volume of solution taken as a platform for the adsorption experiments is called equilibrium concentration and Co is called initial concentration of Metal ions present in the solution.

Adsorption Efficiency can be calculated in percentage by the equation.

$$\text{Removal efficiency} = \frac{C0 - Ce}{C0} \times 100 \quad (2)$$

Here C_0 and $C_{e\,stand}$ for the initial and equilibrium concentrations of the heavy metal ion such as Lead in water media.[12]

For a better understanding of the kinetic mechanism that affects the adsorption of heavy metal ions, and to understand the practical utility of adsorbent synthesized different adsorption models were employed. Kinetic models practiced for the same purpose are pseudo-first-order and pseudo-second-order kinetics. The Curve fitting studies are used for the understanding of the rate of the reaction. The rate expression represents pseudo first order kinetics and the linear equation of pseudo second order kinetics is.

$$q_t = q_e\left(1 - e^{-k_1 t}\right) \quad (3)$$

$$\frac{t}{qe} = \frac{1}{K2qe\,\hat{}\,2} + \frac{1}{K2}\,t \quad (4)$$

q_t and q_e are the amount of adsorbed metal ions adsorbed at a given time t and at equilibrium conditions. The rate constant for the pseudo-first-order kinetic model is k1. K_1 and K_2 are rate constants for pseudo-first-order and second-order kinetic models [13-14].

For a better understanding of the nature of adsorption, different isotherm models are also suggested. Freundlich isotherm, Langmuir isotherm, and Sips isotherm models were employed for this purpose. The Freundlich adsorption isotherm can be represented by the equation.

$$q_e = K_F C_e^{\frac{1}{n}} \quad (5)$$

Here C represents the concentration of heavy metal ions present in the solution taken for analysis. 1/n is called heterogeneity constant, and its value varies between zero to a maximum value of one. K_F is generally a function that depends on the temperature and energy changes during the adsorption process [15-16].

Langmuir accounts for the unimolecular adsorption and considers each surface site of adsorbent to be independent and they are not interacting with each other. Kinetic expression for drawing the Langmuir model is

$$q_e = \frac{q_m\, b\, C_e}{1 + b\, C_e} \quad (6)$$

here b corresponds to the Langmuir constant for the unimolecular process.

The Sips Isotherm model is a three-parameter model suggested by the combination of the rules of Langmuir and Freundlich adsorption isotherms. Sips isotherm fitting is done according to the expression,

$$q_e = qm \times \frac{(K\,Ce)\hat{}n}{[1 + (K \times C_e)\hat{}n]} \quad (7)$$

Here qe is the number of adsorbed molecules at equilibrium condition, qm is the Maximum adsorption capacity, K is called the sips isotherm constant, and n is the sips model exponential [17-18].

RESULTS AND DISCUSSION

Fig. 1 shows the XRD pattern of the prepared α- MnO_2 nanorods. All the peaks can be indexed to the pure tetragonal phase of α-MnO_2 (JCPDS No. 44-0141) with lattice constants of a = 0.982 nm and c = 0.286 nm. No peaks for other types of manganese oxides are observed, indicating that the as-prepared products are phase-pure α-MnO2 nanorods. The sharp diffraction peaks at 13^0, 18^0, 29^0, 38^0, 42^0, 50^0, 57^0, and 61^0 are characteristic ones for the α-MnO2 phase and no other impurity peak was observed to reveal that the products are well crystalline. In addition, it is worth noting that the relative intensity of the (110) peak and (220) are much stronger than that of the standard JCPDS card. However, the relative intensities of other diffraction peaks are comparable to those of the standard JCPDS card [21-24]. The crystallite size of particles was deduced from the Debye– Scherrer equation:

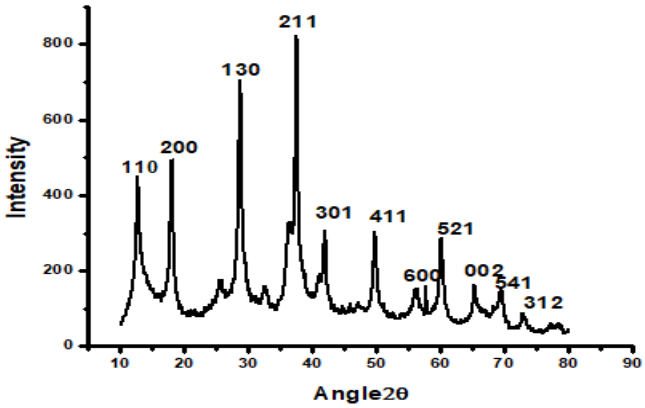

Fig. 1. XRD pattern of the as-prepared α MnO_2 nanorods

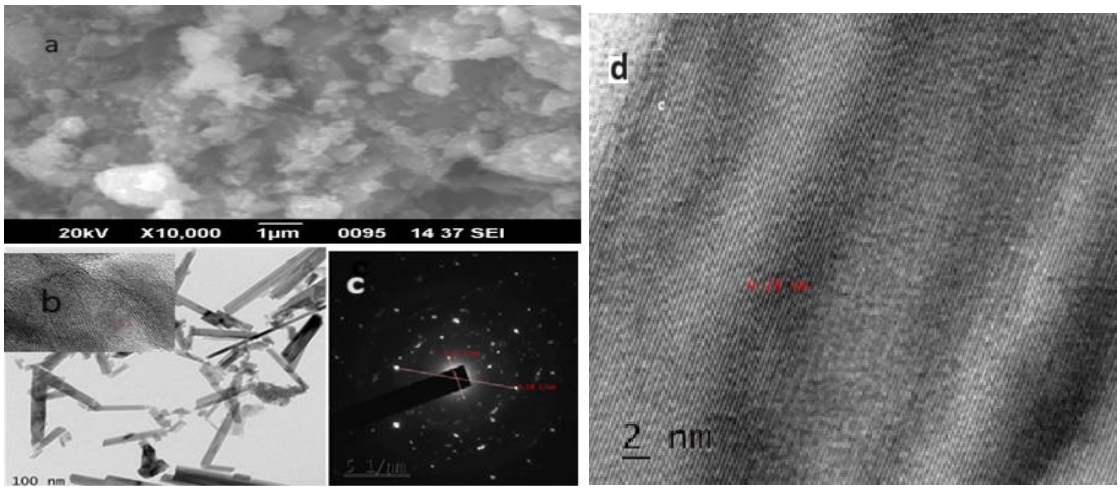

Fig. 2. (a) SEM images of the as-prepared α-MnO_2 nanorods;(b) HRTEM images of the α-MnO_2 nanorods the inset shows images of 2nm; (c) corresponding SAED pattern of the α-MnO_2 nanorods. (d) an individual rod demonstrates that the nanorod has uniform lattice fringes.

$$D = 0.9\lambda/\beta \cos\theta \quad (8)$$

where λ is the wavelength of the X-ray used for the analysis, D is the crystalline size, β is the full width at half-maximum of each peak for calculation, and θ is the Bragg's angle in radians. The average crystallite size obtained is 14.83nm.

The morphology of α-MnO_2 nanorods was examined by SEM images, given in Fig. 2(a). The image shows the formation of agglomerated nanorods that are densely and randomly aligned. For a more clear understanding, TEM images were also obtained. Fig. 2(b) The insets show the TEM image of a single nanorod structure with 2 nm length Fig. 2(c) which reveals the SAED pattern which also suggests that the nanorods grow along the (001) direction (c axis). The TEM image of part of an individual rod demonstrates that the nanorod has uniform lattice fringes as shown in Fig. 2(d). The lattice spacing is calculated to be 0.28 nm (Fig. 2(d)), which corresponds to the (110) plane of α-MnO_2 (JCPDS No. 44-0141) [21-24]

The result of the FTIR Spectrum of leaf extract shows several absorption bands at 540 cm^{-1},1006 cm^{-1},1230 cm^{-1},1382 cm^{-1},1584 cm^{-1},2846 cm^{-1},2917 cm^{-1},3272cm^{-1} respectively (Fig. 3). The band at 540cm^{-1} is due to the C-H bond in aliphatic compounds,1006cm-1 is attributed to C-O stretching vibrations in alcohols ethers or esters,1230cm^{-1} indicates the presence of C-O stretching vibrations,1382cm^{-1} is often associated with C-H bending vibrations. C=C stretching indicated by 1584cm^{-1},2846cm^{-1} and 2917cm^{-1} are characteristic of C-H stretching vibrations'-H stretching vibrations are indicated by 3272cm^{-1}. All these point out the occurrence of various functional groups in the extract such as O–H,

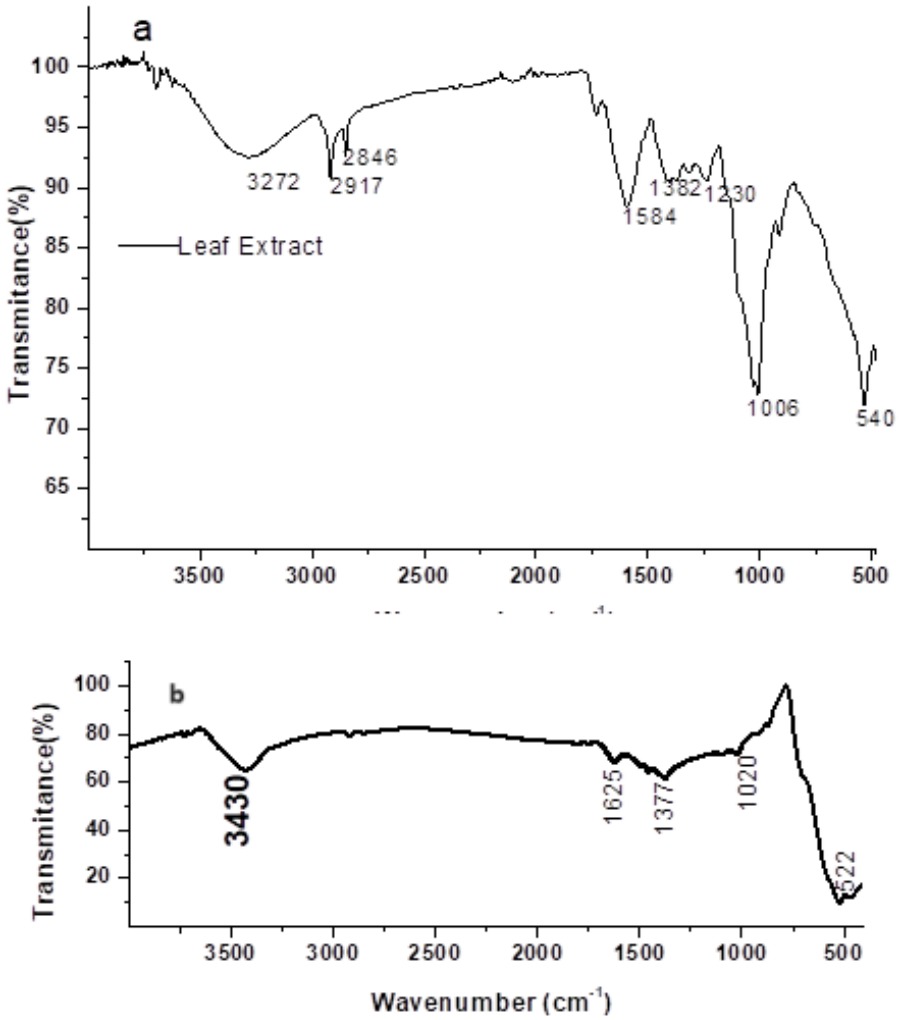

Fig. 3. The FT-IR spectrum of (a) Coleus amboinicus leaf extract (b)α MnO2 nanorod.

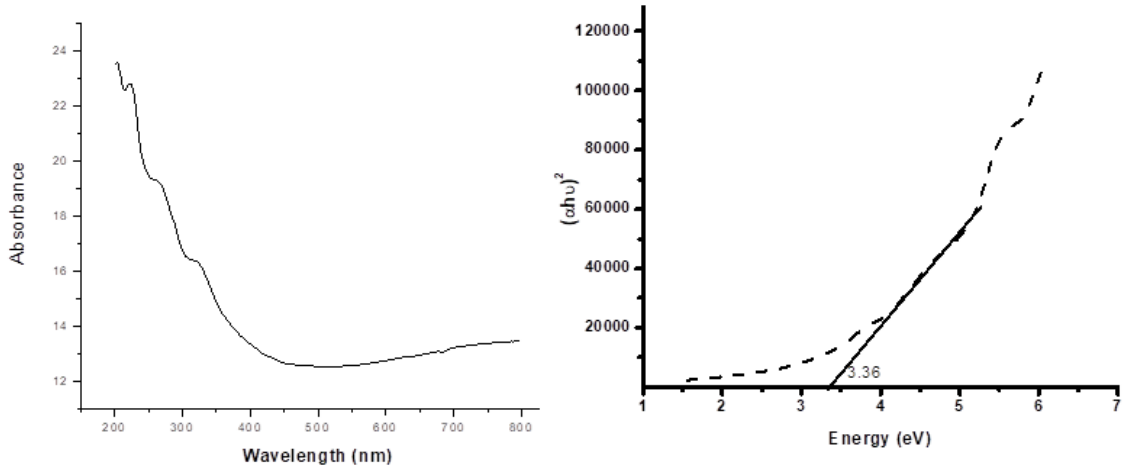

Fig. 4. The UV-Vis spectrum of (a)α MnO$_2$ nanorod (b) Tauc Plot

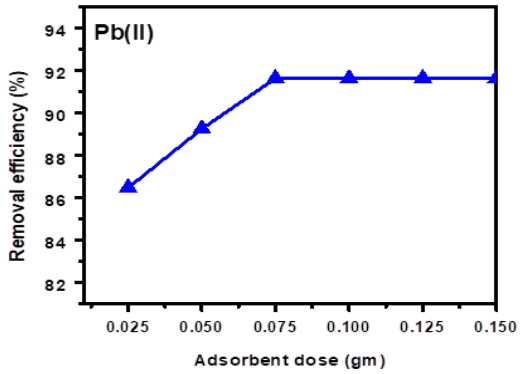

Fig. 5. Effect of adsorbent dose on adsorption of Pb(II) on αMnO2

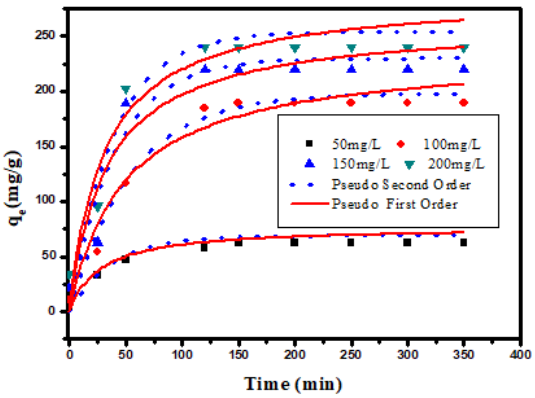

Fig. 6. Kinetic models for adsorption of αMnO2 for Pb(II) ions

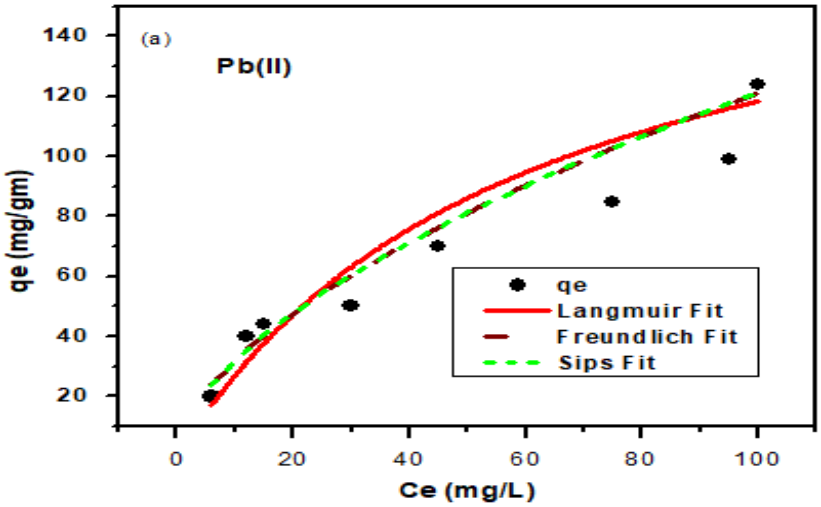

Fig. 7. Adsorption isotherm models of αMnO2 for Pb(II) ions

C–H, CO_2, C=O, C=C, N–H, and C–O. On the other hand, green-synthesized MnO_2 nanorod not only presented the characteristic FTIR signal for Mn–O at about 522 $cm^{-1,}$ and 1020cm^{-1} arises due to metal oxygen stretching vibrations but also showed other FTIR signals for O–H, C=O, C–O. Hence, these observations demonstrated that green-synthesizedα -MnO2 nanorods are entirely capped with the biologically active Phyto molecules of plant leaf extract having such functional groups [25].

The optical absorption spectra of MnO_2 nanoparticles in the range of 200-800nm are shown in Fig. 4. The value of band gap energy (Eg) was estimated by the method proposed by Wood and Tauc, according to the following equation

$$(\alpha h\nu)\ \alpha\ (h\nu\text{-}Eg)^{n} \quad (9)$$

Where Eg is the band gap energy, α is the absorption coefficient, n = ½ for direct transition, and n = 2 for indirect transition. The MnO_2 shows absorption at wavelengths of 330 nm with bandgap values of 3.36eV [26-28].

Adsorption Study.

The as-synthesized manganese oxide was used as an adsorbent for Pb (II) removal. Fig. 6 shows the effect of contact time on the adsorption of Pb (II). The effect of the adsorbent dose on adsorption was carried out by various doses of the α MnO_2 the results are shown in Fig 5. The adsorption efficiency of Pb (II) increased gradually with increasing of the adsorbent dose from 0.02 to 0.1 gm. Moreover, it was found that when the adsorbent dose was further increased by 0.10mg, the adsorption efficiency was almost unchanged [29]. From this when the adsorbent dose is more than 0.10gm, the adsorption equilibrium is reached, and the adsorption trend to stabilization. Therefore, the

Table. 1 The adsorption parameters for Pseudo first-order and second-order kinetics of Pb(II) on MnO_2

Metal ion	q_e(mg/g)	Pseudo-first-order				Pseudo-second-order			
	Exp	q_e(mg/g)	k_1/min	R^2	χ^2	q_e(mg/g)	k_2 min^{-1}	R^2	χ^2
	90.23	81.25	0.01	0.96	0.27	91.87	0.6x10^{-4}	0.97	0.88
Pb(ll)	139.85	105.45	0.01	0.98	0.14	138.28	0.2x10^{-4}	0.99	0.74

Table. 2 Isotherm parameters for the adsorption of Pb(ll) on αMnO$_2$.

Isotherm Parameters	Pb(II)
Langmuir	
R^2	0.979
χ^2	1.2
Freundlich	
R^2	0.981
χ^2	1.8
Sips	
R^2	0.99
χ^2	0.1

optimum dose of the nano αMnO$_2$ was 0.01gm in this study [27], [30].

The kinetics of the adsorption study was done for different time intervals. As expected, the ion removal increased linearly with the contact time, and the adsorption efficiency for Pb (II) was 90% at time 120 min was observed. The fitting of the experimental kinetic data to the pseudo-first- and pseudo-second-order models is presented in Fig. 6 and the Correlation between the experimental data and the linear behavior is described by Table 1. These observations were in accord with the kinetic data described for inorganic adsorbents [6], [7], [31].

Even when the R^2 values for the adsorption kinetics of Pb (II) are lower in the pseudo-first-order model than in the pseudo-second-order model. The closeness of qe values might suggest that the kinetic of these metallic ions can be better described by a non-linear process. The calculated correlation coefficients are less than 0.963 for the first-order kinetic model, whereas the values of the correlation coefficient are greater than 0.996 for the pseudo-second-order kinetic model. Therefore, the adsorption kinetics could be well explained by the pseudo-second-order kinetic model for the prepared nano αMnO$_2$.

Adsorption isotherms

Three kinds of isotherms' equations were tested to fit the experimental data such as Langmuir, Freundlich, and Sips isotherm equations shown in Fig. 7.: The isotherm constants were calculated using nonlinear regression analysis. The values are summerised in Table 2 of R^2 and χ^2 showed that the adsorption of Pb(ll) was best fitted with the Sips isotherm model over the various concentrations studied. Sips isotherm model is a blend of Langmuir and Freundlich adsorption isotherm models. The higher q_{max} value obtained for Sips is attributed to the fact that at higher concentrations Sips favors the Langmuir model while at lower concentrations it favors the Freundlich model [32], [33].

CONCLUSION

In this work, we investigated the adsorption behavior of the biosynthesized nano metal oxide αMnO$_2$. Which is a better candidate for the efficient sequestration of pollutants such as lead from the aqueous media. 0.1 g of adsorbent called αMnO$_2$ was used for the purpose. Adsorption kinetic measurements showed that the adsorption procedure follows a pseudo-second-order kinetics. Isotherm analyses were also carried out using three different isotherm models through suitable fitting equations. Out of all Sips fit better than other isotherms which is clear from the regression analysis performed. The same further suggests the homogeneous monolayer adsorption of Pb^{2+} ions on the surface of the adsorbent. αMnO$_2$ is then considered a better catalyst for the treatment of wastewater containing lead.

CONFLICTS OF INTEREST

There are no conflicts of interest to declare.

ACKNOWLEDGMENTS

We greatly acknowledge DST-SAIF Cochin and CLIF, Kariavattom for their help during the analysis of samples.

REFERENCE

[1] S. Ahmadi and C. Izanloo, "Biosynthesis of iron oxide nanoparticles at different temperatures and its application for the removal of Zinc by plant mediated nanoparticle, as an eco-friendly nanoadsorbent," Results Chem, vol. 6, Dec. 2023, doi: 10.1016/j.rechem.2023.101192.

[2] S. Chakrabarty, M. A. Mahmud, M. H. Ara, and S. Bhattacharjee, "Development of a platform for removal of iron (III) ions from aqueous solution using CuO nanoparticles," Journal of Water and Environmental Nanotechnology, vol. 6, no. 1, pp. 41-48, 2021, doi: 10.22090/jwent.2021.01.004.

[3] A. P. Shende and N. Das, "Green synthesis of iron nanoparticles using bioflocculant extracted from okra (Abelmoschus esculentus (l) moench) and its application towards elimination of toxic metals from wastewater: A statistical approach," Journal of Water and Environmental Nanotechnology, vol. 6, no. 4, pp. 338-355, Sep. 2021, doi: 10.22090/jwent.2021.04.005.

[4] M. Sindhudevi1, S. Srinivasan, B. Karthekiyan1, and A. Muthuvel, "Green synthesis and characterization of Selenium/Zirconium bimetallic nanoparticles using Cinnamomum camphora leaf extract and their photocatalyst and anticancer activity," J. Water Environ. Nanotechnol, vol. 8, no. 4, pp. 417-441, 2023, doi: 10.22090/jwent.2023.04.008.

[5] M. Rabaa, A. Aridi, G. Younes, and R. Awad, "Samarium doped Mg0.33 Ni0.33 Co0.33 Fe2 O4 Nanoparticles for the Removal of As (III) and Pb (II) Heavy Metal Ions," Journal of Water and Environmental Nanotechnology, vol. 8, no. 4, pp. 357-368, Nov. 2023, doi: 10.22090/JWENT.2023.04.003.

[6] K. Gupta, P. Joshi, R. Gusain, and O. P. Khatri, "Recent advances in adsorptive removal of heavy metal and metalloid ions by metal oxide-based nanomaterials," Coord Chem Rev, vol. 445, p. 214100, Oct. 2021, doi: 10.1016/j.ccr.2021.214100.

[7] W. Weilong and F. Xiaobo, "Efficient removal of Cr(VI) with Fe/Mn mixed metal oxide nanocomposites synthesized by a grinding method," J Nanomater, vol. 2013, 2013, doi: 10.1155/2013/514917.

[8] H. Chen and J. He, "Facile synthesis of monodisperse manganese oxide nanostructures and their application in water treatment," Journal of Physical Chemistry C, vol. 112, no. 45, pp. 17540-17545, Nov. 2008, doi: 10.1021/jp806160g.

[9] N. Ponomarev and M. Sillanpää, "SYNTHESIS OF NOVEL CELLULOSE BASED NANOCOMPOSITES BY GREEN METHODS AND THEIR POSSIBLE USE AS ADSORBENTS."

[10] H. Zhang et al., "Efficient removal of Pb(II) ions using manganese oxides: The role of crystal structure," RSC Adv, vol. 7, no. 65, pp. 41228-41240, 2017, doi: 10.1039/c7ra05955h.

[11] Y. Huang, X. Luo, C. Liu, S. You, S. Rad, and L. Qin, "Effective adsorption of Pb(ii) from wastewater using MnO2 loaded MgFe-LD(H)O composites: adsorption behavior and mechanism," RSC Adv, vol. 13, no. 28, pp. 19288-19300, Jun. 2023, doi: 10.1039/d3ra03035k

[12] I. Sheet, A. Kabbani, and H. Holail, "Removal of heavy metals using nanostructured graphite oxide, silica nanoparticles and silica/graphite oxide composite," in Energy Procedia, Elsevier Ltd, 2014, pp. 130-138. doi: 10.1016/j.egypro.2014.06.016.

[13] T. R, "Metal Oxide Nano-particles as an Adsorbent for Removal of Heavy Metals," Journal of Advanced Chemical Engineering, vol. 5, no. 3, 2015, doi: 10.4172/2090-4568.1000125.

[14] A. M. Mahmoud, F. A. Ibrahim, S. A. Shaban, and N. A. Youssef, "Adsorption of heavy metal ion from aqueous solution by nickel oxide nano catalyst prepared by different methods," Egyptian Journal of Petroleum, vol. 24, no. 1, pp. 27-35, Mar. 2015, doi: 10.1016/j.ejpe.2015.02.003.

[15] P. N. Dave and L. V. Chopda, "Application of iron oxide nanomaterials for the removal of heavy metals," Journal of Nanotechnology, vol. 2014. Hindawi Publishing Corporation, 2014. doi: 10.1155/2014/398569.

[16] N. Ghosh, S. Das, G. Biswas, and P. K. Haldar, "Review on some metal oxide nanoparticles as effective adsorbent in wastewater treatment," Water Science and Technology, vol. 85, no. 12. IWA Publishing, pp. 3370-3395, Jun. 15, 2022. doi: 10.2166/wst.2022.153.

[17] G. M. Al-Senani and F. F. Al-Fawzan, "Study on Adsorption of Cu and Ba from Aqueous Solutions Using Nanoparticles of Origanum (OR) and Lavandula (LV)," Bioinorg Chem Appl, vol. 2018, pp. 1-8, Sep. 2018, doi: 10.1155/2018/3936178.

[18] U. O. Aigbe, R. Maluleke, T. C. Lebepe, O. S. Oluwafemi, and O. A. Osibote, "Rhodamine 6G Dye Adsorption Using Magnetic Nanoparticles Synthesized With the Support of Vernonia Amygdalina Leaf Extract (Bitter Leaf)," J Inorg Organomet Polym Mater, 2023, doi: 10.1007/s10904-023-02639-3.

[19] P. B. Sreelekshmi, R. R. Pillai, and A. P. Meera, "Evaluation of Antimicrobial Activity of Bio Synthesised Zinc Oxide Nanoparticles Using Morinda umbellata Leaf Extract," ECS Trans, vol. 107, no. 1, pp. 15953-15964, Apr. 2022, doi: 10.1149/10701.15953ecst. [20] M. Khalatbary, M. H. Sayadi, M. Hajiani, M. Nowrouzi, and S. Homaeigohar, "Green, Sustainable Synthesis of γ-Fe2O3/MWCNT/Ag Nano-Composites Using the Viscum album Leaf Extract and Waste Car Tire for Removal of Sulfamethazine and Bacteria from Wastewater Streams," Nanomaterials, vol. 12, no. 16, Aug. 2022, doi: 10.3390/nano12162798.

[21] H. Wang, Z. Lu, D. Qian, Y. Li, and W. Zhang, "Single-crystal α-MnO2 nanorods: Synthesis and electrochemical properties," Nanotechnology, vol. 18, no. 11, Mar. 2007, doi: 10.1088/0957-4484/18/11/115616.

[22] S. Devaraj and N. Munichandraiah, "Surfactant stabilized nanopetals morphology of α-MnO 2 prepared by microemulsion method," Journal of Solid State Electrochemistry, vol. 12, no. 2, pp. 207-211, Feb. 2008, doi: 10.1007/s10008-007-0364-7.

[23] L. Sanchez-Botero, A. P. Herrera, and J. P. Hinestroza, "Oriented growth of α-MnO2 nanorods using natural extracts from grape stems and apple peels," Nanomaterials, vol. 7, no. 5, May 2017, doi: 10.3390/nano7050117.

[24] Z. K. Ghouri et al., "High-efficiency super capacitors based on hetero-structured α-MnO2 nanorods," J Alloys Compd, vol. 642, pp. 210-215, Sep. 2015, doi: 10.1016/j.jallcom.2015.04.082.

[25] S. A. Khan, S. Shahid, B. Shahid, U. Fatima, and S. A. Abbasi, "Green synthesis of MNO nanoparticles using abutilon indicum leaf extract for biological, photocatalytic, and adsorption activities," Biomolecules, vol. 10, no. 5, May 2020, doi: 10.3390/biom10050785.

[26] H. Yu and L. Zheng, "Manganese dioxide nanosheets as an optical probe for photometric determination of free chlorine," Microchimica Acta, vol. 183, no. 7, pp. 2229-2234, Jul. 2016, doi: 10.1007/s00604-016-1857-9.

[27] N. Ghosh, S. Das, G. Biswas, and P. K. Haldar, "Review on some metal oxide nanoparticles as effective adsorbent in wastewater treatment," Water Science and Technology, vol. 85, no. 12. IWA Publishing, pp. 3370-3395, Jun. 15, 2022. doi: 10.2166/wst.2022.153.

[28] A. V. Soldatova, G. Balakrishnan, O. F. Oyerinde, C. A. Romano, B. M. Tebo, and T. G. Spiro, "Biogenic and Synthetic MnO2 Nanoparticles: Size and Growth Probed with Absorption and Raman Spectroscopies and Dynamic Light Scattering," Environ Sci Technol, vol. 53, no. 8, pp. 4185-4197, Apr. 2019, doi: 10.1021/acs.est.8b05806.

[29] S. Lotfi, B. Aslibeiki, and M. Zarei, "Efficient pb(Ii) removal from wastewater by teg coated fe3 o4 ferrofluid," Journal of Water and Environmental Nanotechnology, vol. 6, no. 2, pp. 109-120, Mar. 2021, doi: 10.22090/jwent.2021.02.002.

[30] J. Yang et al., "Nanomaterials for the removal of heavy metals from wastewater," Nanomaterials, vol. 9, no. 3. MDPI AG, Mar. 01, 2019. doi: 10.3390/nano9030424.

[31] Raveendra RS, "Preparation of MnO2 nanoparticles for the adsorption of environmentally hazardous malachite green dye." [Online]. Available: www.ijaiem.org

[32] G. M. Al-Senani and F. F. Al-Fawzan, "Study on Adsorption of Cu and Ba from Aqueous Solutions Using Nanoparticles of Origanum (OR) and Lavandula (LV)," Bioinorg Chem Appl, vol. 2018, pp. 1-8, Sep. 2018, doi: 10.1155/2018/3936178.

[33] U. O. Aigbe, R. Maluleke, T. C. Lebepe, O. S. Oluwafemi, and O. A. Osibote, "Rhodamine 6G Dye Adsorption Using Magnetic Nanoparticles Synthesized With the Support of Vernonia Amygdalina Leaf Extract (Bitter Leaf)," J Inorg Organomet Polym Mater, 2023, doi: 10.1007/s10904-023-02639-3.